Microscale concave interfaces for reflective displays generate concentric rainbows

Jacob Rada^a, Haifeng Hu^b, Lyu Zhou^a, Jing Zeng^c, Haomin Song^a, Xie Zeng^a, Shakil Shimul^d, Wen Fan^e, Qiwen Zhan^b, Wei Li^d, Limin Wu^c, Qiaoqiang Gan^{a,*}

^a Department of Electrical Engineering, The State University of New York at Buffalo, Buffalo, NY 14260
^b School of Optical-Electrical and Computer Engineering, University of Shanghai for Science and Technology, Shanghai 20093, China
^c Department of Materials Science, Fudan University, Shanghai 200433, China
^d Department of Chemical Engineering, Texas Tech University, Lubbock, TX 79409, USA
^e School of Materials Science and Engineering, Hubei University, Wuhan, Hubei 430062, China qqgan@buffalo.edu

Abstract: Structural color utilizing microscale concave interfaces has been reported in several publications, but the explanation is currently incomplete. Within this work, the physics behind this coloration technique is clarified using multiple light sources and simulations. © 2022 The Author(s)

1. Main Text

Active display electronics experience the largest battery drain when powering the screen. Reflective display technologies that require no active illumination can provide significant relief, and improve the battery life of the device. This concept has already been implemented in devices such as: electronic papers (E-papers, which use electrophoretic motion of ink particles), electrowetting devices utilizing water/oil droplets, and interferometric modulators. While the battery saving features of these devices is novel, they are limited in use due to their poor screen brightness. Within this work(1), we report an experimental observation of multiple concentric circular rainbows from reflective microscale concave interfaces (MCI). These colorful rainbows are produced by the reflection of optical rays within polymer-embedded microspheres. By partially embedding uniform diameter microspheres into a transparent tape (the embedded depth is roughly half the diameter of the microsphere), total internal reflection occurs at the sphere-tape interface, and generates the vivid visible rainbow colors in the far field. The mechanism behind this coloration phenomenon must be clarified, as the MCI samples can be useful when

implemented as commercially viable passive display technologies.

When light travels from a material with a high refractive index to a material with a low refractive and is simultaneously incident on the low index material at an angle larger than the critical angle, θ_c , total internal reflection (TIR) will occur. The microspheres used within our MCI are composed of polystyrene (PS), which has a refractive index of 1.6. Total internal reflection occurs because there is a large refractive index difference between the spheres and surrounding air (n_{air}=1.0). This work's characterization setup is shown in Fig. 1A, showing a light source illuminating the MCI sample

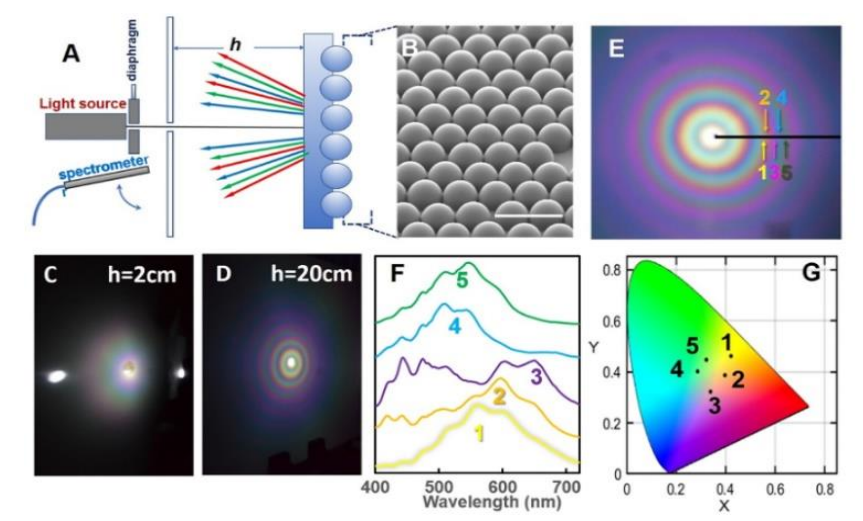


Figure 1. (A) MCI optical characterization setup; (B) Sem image of microspheres embedded within tape. The scale bar is $20\mu m$; (C), (D) Rainbow colors of $10\mu m$ PS MCI at an observation distance, h, of 2cm (C), and 20cm (D); (E) Rainbow rings of $10\mu m$ PS MCI at a distance of 30cm. Five spectral measurement points are indicated with differently colored arrows; (F) Spectra measured from E; (G) CIE points converted from the spectra measured in F

(of which an SEM is shown in Fig. 1B), and a fiber-based spectrometer that is moved horizontally to measure the resulting spectrum. When the MCI-observer distance (h) is adjusted for the 10µm PS sample, differing rainbow

patterns are visible, as shown in figs. 1C and 1D. This observation was not made in either of the preceding works [2,

3], and represents a key finding in the understanding of the physics. When placed 30cm away from the board, **Fig. 1E**, the full rainbow rings are shown, and the spectral measurement points used in **Fig. 1F** are indicated with arrows. The spectra were then directly translated into a point on the CIE chart, as seen in **Fig. 1G**.

When a light source is normally incident on the MCI, only certain spatial angle ranges for the output rays with m=2 and m=3 are possible, as plotted in Fig. 2A. Because of the symmetrical properties of the sphere, light is able to enter on either the right or left edge, and propagates along the concave sphere/air interface via TIR in the clockwise/anti-clockwise direction. For $\theta_{\text{ext}}=15^{\circ}$, as seen in **Fig. 2B**, three rays exist and are marked by the colored dots in Fig. 2A. Two of these rays experience TIR twice, but enter and escape from the opposite edge (i.e., m=2). They also interfere with each other under the given conditions. For the large output angles, shown in **Fig. 2C**, two rays experience a different amount of TIR, but enter and exit on the same side, which is the multi-bouncing TIR superposition proposed by ref. 2. Both ref. 2, and ref. 3

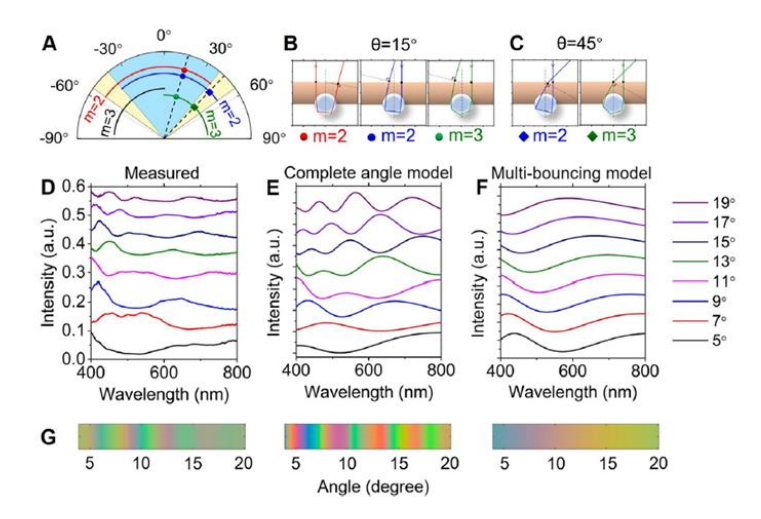


Figure 2. (A) Output angle ranges for reflected rays generated from model. The dashed lines represent output angles of 15° and 45° . The solid blue/red curve represent rays that propagate in the clockwise/anti-clockwise direction with m=2 bounces, while the green/black solid curve represent rays that propagate in the clockwise/anti-clockwise direction with m=3 bounces. (B, C) Modeled trajectories of the light rays with an output angle of (B) $\Theta=15^\circ$, and (C) 45° , respectively. (D) Measured angular spectra of the $10\mu m$ PS MCI sample in the far field (E, F), Simulation of the far field interference pattern using the (E) angle-dependent interference method, and (F) the multi-bouncing interference method, respectively. (G) Color bar generated from the measured and simulated spectra shown in (D-F). The measured and complete angle-dependent model spectra create similar banded color bars, whereas the multi-bouncing model only shows a gradual color shift.

reported coloration under incident angles of 40° to 50° , however, our modeling suggests that the smaller output angle regions (the shaded blue region between \pm 39.7°) should be considered.

Within ref. 2, the one-to-one correspondence between the spectral features and the observed color was missing. We characterized the angle-dependent reflection spectra within an angular range of 3° to 20° (8 spectra shown in Fig. 2D). The corresponding spectra using our complete angle-dependent model, and the exclusive multi-bouncing TIR interference of ref. 2 are plotted in Fig. 2E and Fig. 2F, respectively. There is a clear agreement between our measured results, and the results of our complete angle-dependent model. On the contrary, the measured results do not match well with the simulation using the multi-bouncing model. The measured and modeled spectra were then converted into colors perceptible to the human eye, and plotted in Fig. 2G. The observed multiple rainbow pattern was only generated using the complete angle model, which is significantly different from the pattern produced by ref. 2's model.

By combining experimental data, and ray-optics simulations, our work demonstrates the merits of the proposed complete angle-dependent model. Our as-fabricated MCI is a capable passive reflective display technology, producing numerous different colors at different viewing distances and diameters. The colors were experimentally measured using a fiber optic spectrometer, and directly compared to the results of several different models. With this better understanding of the physics behind this optical phenomena, our MCI structures can be used to produce passive display technologies. These technologies can include: road signs, NIR targets for LiDAR applications, and children's toys.

3. References

- [1] J. Rada, et al., Multiple concentric rainbows induced by microscale concave interfaces for reflective displays, Applied Materials Today 24, 101146 (2021).
- [2] A.E. Goodling, et al., Colouration by total internal reflection and interference at microscale concave interfaces, Nature 566, 523 (2019).
- [3] W. Fan, et al., Iridescence-controlled and flexibly tunable retroreflective structural color film for smart displays, Sci. Adv. 5, eaaw8755 (2019).